Springer

KSME

Journal of Mechanical Science and Technology 33 (8) (2019) 3913~3925
www.springerlink.com/content/1738-494x(Print)/1976-3824(Online)
DOI 10.1007/s12206-019-0736-9

A new method of enhancing heat transfer in sudden expansion channel using vortex generators with toe-out and toe-in configurations by acquiring perquisites of recirculation and secondary vortex flow †

S. Ramanathan[1], M. R. Thansekhar[2,*], P. Rajesh Kanna[3] and Prem Gunnasegaran[4]

[1]*Department of Mechanical Engineering, Kumaraguru College of Technology, Coimbatore 641035, Tamil Nadu, India*
[2]*Department of Mechanical Engineering, K.L.N. College of Engineering, Madurai 630612, Tamil Nadu, India*
[3]*Department of Mechanical Engineering, College of Engineering and Computing, Alghurair University, Dubai, UAE*
[4]*Department of Mechanical Engineering, College of Engineering, Universiti Tenaga Nasional, Kajang, Malaysia*

(Manuscript Received August 21, 2018; Revised March 8, 2019; Accepted April 14, 2019)

Abstract

The relative positions of leading edges and trailing edges of rectangular vortex generators (VG) in the winglet form play a crucial role in modifying thermal and hydraulic boundary layers thereby affecting the heat transfer augmentation and pressure drop in a sudden expansion channel having expansion ratio (ER) 2:1. A numerical simulation was carried out for solving the momentum and energy equations of a three dimensional vortex- laminar flow (Reynolds number < 190) with a finite volume method based commercial code FLUENT 16.2. Reynolds number, angle of attack and VG configuration have been considered as influential parameters affecting the thermo-hydraulic performance of the sudden expansion channel due to the combined effect of primary recirculation and secondary vortex flow. The heat transfer enhancement along with corresponding pressure drop penalty was compared for the toe-out and toe-in configurations at various Reynolds (Re) numbers and angle of attacks (β). Eventually irrespective of configurations, rectangular winglet VGs are found to have better overall performance at β = 30° and β = 45° in both toe-out and toe-in configurations due to strong secondary vortex flow.

Keywords: Sudden expansion; Laminar flow; Vortex generators; Heat transfer enhancement

1. Introduction

Convective heat transfer enhanced through a large number of techniques has been the subject of study seen in literature for realizing better performance of devices dissipating heat as part of working. Active, passive and combination of both are the major classifications of heat transfer augmentation techniques according to Bergles [1, 2]. As passive methods do not require any external power or energy for enhancing heat transfer and make use of a secondary heat transfer surfaces like plain, louvered, slit, wavy, annular, longitudinal and serrated fins or fluid additives to increase effective thermal conductivity of fluid [3-5], and for reducing the energy of thermodynamic system [6], it is the most sought after method for increasing the heat transfer rate. Flow detachment in sudden expansion, and vortices created by VGs and parameters affecting these two were seen as the cause for inducing a drag in the engineering system [7, 8]. Later flow detachment and vortices were viewed as agents for the promotion of heat transfer enhancement. Researchers all over the world in last two decade have paid considerable attention to sudden expansion as one of the classical geometries due to its wide range of application comprising electronic equipment, cooling of turbine blades, combustion chamber, heat exchanger, refrigeration and air-conditioning system, solar collector and nuclear reactors [9-17]. Cherdron et al. [18] came up with a breakthrough conclusion almost four decades back that, at fixed ER, decreasing aspect ratio of sudden expansion channel results in a higher critical Re number due to side wall proximity. Ouwa et al. [19] found the transition of primary vortex flow from two dimensional into three dimensional at a higher Re number through loss of its stable growth with Re number. Chiang et al. [20] proposed that at aspect ratio above 12, the flow is predominantly two dimensional on center plane of a sudden expansion channel and side walls had lost its influence completely on this mid plane. Zhang et al. [21] reported increasing Re number and heat flux accompany heat transfer enhancement which was maximum around the reattachment point and increase in reattachment length. Kanna et al. [22] predicted

*Corresponding author. Tel.: +91 452 2091965, Fax.: +91 452 2090070
E-mail address: thansekhar@yahoo.com
† Recommended by Associate Editor Seongwon Kang

enhancement of heat transfer in both fluid and solid region in the presence of nanoparticle in base fluid. Nu was also seen having a peak and asymptotic value within the recirculation region and in the downstream respectively. Togun et al. [23] found increase in the size of primary recirculation zone with increase in Re number and ER, and volume fraction of nanoparticle in base fluid had a significant effect on increasing heat transfer due to nanoparticle heat transport. Kimouche et al. [24] also confirmed increase in the volume fraction and Re number increase the heat transfer rate, whereas for Re > 5000, volume fraction did not affect size of primary recirculation zone considerably. Sayed ahmed et al. [3] compared the heat transfer characteristics of wing-shaped tube heat exchanger with circular and elliptical tube heat exchanger and concluded that effectiveness and efficiency index of wing-shaped tube heat exchanger have maximum value at zero angle of attack, and efficiency index of wing-shaped tube heat exchanger at zero angle of attack is maximum compared to circular and elliptical tube heat exchanger at all angle of attack. In connection with their previous work, Syed ahmed et al. [4] investigated the effect of angle of attack and cone angle of wing-shaped tubes on flow characteristics and concluded that arrangement with zero angle of attack has the least air flow pressure drop co-efficient and pumping power whereas the arrangement with cone angle = 90° has the highest value of pressure drop coefficient and pumping power in the Reynolds number range considered. Gong et al. [25] found heat transfer augmentation could be better if transversal axis of tube is aligned with the leading edge of curved rectangular winglet vortex generators (CRWVGs) and diameter of base arc of VG as larger. Lin et al. [26] conducted the same experiment but with a curved delta winglet vortex generator (CDWVG) and agreed that better heat transfer augmentation could be obtained if the leading edge of CDWVG is offset by a distance equivalent to 5° from transversal axis of pipe in the downstream, and length and height of CDWVG had no significant effect on Nu and friction factor. Wu et al. [27] declared that, with CDWVG, Nu and friction factor increased with increase in fin pitch when tube diameter remained constant and, at the same time, heat transfer enhancement with fin pitch was closely related to Re number and tube diameter. Dang et al. [28] reported the superiority of thermo-hydraulic performance of fin with VG and flow re-distributors to that of plain fin and plain fins with only VG due to secondary flow and reduction in pressure drop penalty, respectively. Flow re-distributors play a crucial role in enhancing heat transfer at small fin spacing irrespective of the geometry of VG with flow-redistributors. Hatami et al. [29] while trying to recover energy from a diesel exhaust using delta winglet vortex generators (DWVGs) at angle of attack of 30° being perceived to be best as seen from findings from literature, concluded that VGs could effectively recover the energy more than 50 % compared to a simple heat exchanger without VGs. Investigation done by Yang et al. [30] lead to their conclusion that the use of delta wing pair in a rectangular channel did not deteriorate the thermal boundary layer as much as the deterioration of hydraulic boundary layer due to the lifting effect of vortices from the bottom wall. Arora et al. [31] optimized the location of DWVG and proposed heat transfer enhancement as maximum when VG was placed around the center of each inline pipe in the stream wise direction as the secondary flow along with shed corner vortex washed away the fluid tapped between the wall of pipe and VG, and was poor in the wake region of each pipe. Pal et al. [32] have reported that heat transfer enhancement was poor when DWVG was located at the rear and relative to that located at the front end, whereas an increase in the angle of attack caused decrease in heat transfer enhancement due to wake formation and weak swirl. Pesteei et al. [33], while enhancing the heat transfer in fin-tube heat exchangers, found DWVG at an angle of attack of 45° increasing the heat transfer coefficient up to 46 % with the accompaniment of an additional pressure drop of 18 %. Li et al. [34] have, in their numerical study of heat transfer on fin-and-tube heat exchanger, explained that rectangular winglet vortex generators (RWVGs) produced more heat transfer than DWVGs for the same angle of attack and, in general, heat transfer enhancement by punched VGs was more effective than mounted ones. Investigation of Bekele et al. [35] was with delta shaped obstacles in solar air heater for higher Re number range. Their conclusion was that the maximum thermo-hydraulic performances could be obtained at an angle of incidence of 30° as the length of the obstacle for the same relative obstacle height as higher than that for the remaining angle of attack holding a large quantity of fluid in the obstacle region thereby enhancing heat transfer.

An indepth study of the relevant literature shows, Zohir et al. [36] as the first to investigate experimentally the combined effect of recirculation arising from a sudden expansion and secondary vortex flow as a result of helical and propeller swirler on heat transfer enhancement in sudden expansion pipe and inferred propeller and helical swirlers as effective in augmenting heat transfer when located nearest to a sudden expansion in downstream and downstream of reattachment region respectively. Zohir et al. [37] extended the earlier work for propeller swirler with different angle of attacks and declared heat transfer enhancement as maximum for swirler with angle of attack of 45°. An elaborative research has been carried out for predicting the influence of rectangular and delta winglet type VGs on heat transfer and fluid flow characteristics in toe-in [25-32] and toe-out [33, 34] configurations separately. A comparison performed by Tian et al. [38] in their numerical study showed overall performance of rectangular winglet pair with toe-out configuration as better than that of toe-in configuration though toe-in configuration had very strong interactive longitudinal vortices to reduce the thickness of thermal boundary layer in the flow domain as it accompanied a tremendous pressure drop. The same feature could be attributed to the performance of delta winglet pair when comparing it to that of rectangular winglet pair especially at higher Re numbers. The above discussions clearly show the perform-

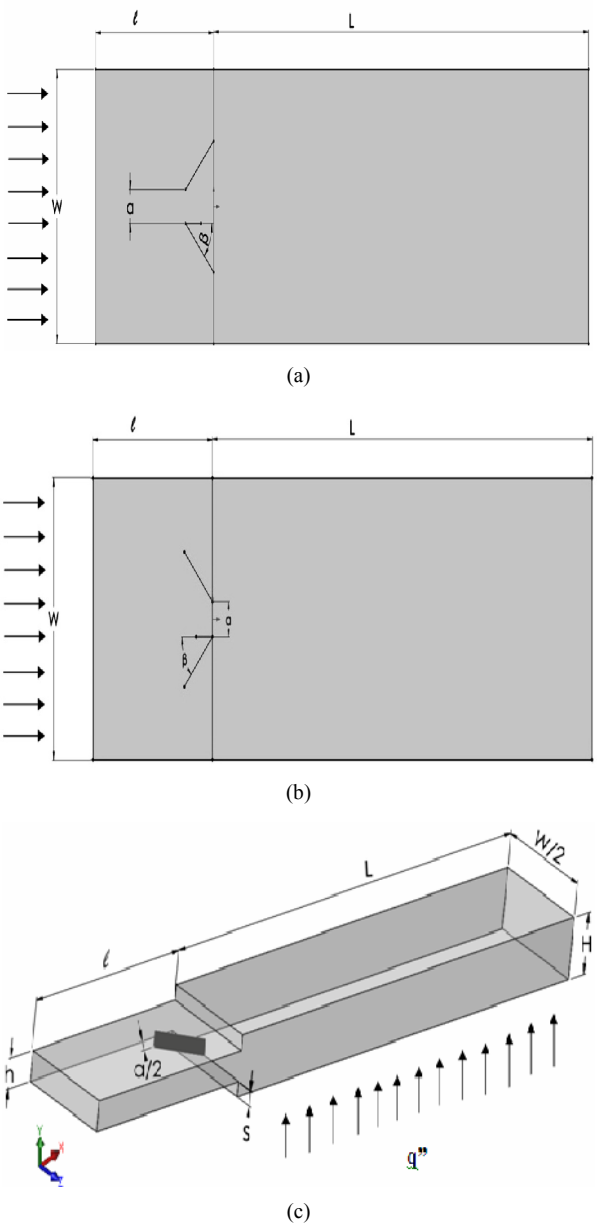

Fig. 1. Physical model in (a) toe-out; (b) toe-in configurations; (c) computational domain of the channel with VG.

ance of only a few works on a comparative study between toe-in and toe-out configurations, and the potentials of combined primary recirculation and secondary vortex flow effects. Thus present numerical study has been taken up for filling up the gap seen in the relevant literatures.

2. Problem statement

Physical model of three dimensional sudden expansion of upstream height 20 mm and downstream height 40 mm with a line of VGs at inlet in both toe-out and toe-in configurations are shown in Figs. 1(a) and (b), respectively. The left bottom corner (viewing from inlet) where backward facing step, bottom wall and sidewall meet, is fixed as the origin of coordinate system. Toe-out and toe-in configurations have been defined with respect to the distance between the trailing edges of VG on the edge of the step of sudden expansion. Rectangular winglet vortex generator of length 40 mm and height 10 mm has been considered for heat transfer enhancement and fluid flow analysis in sudden expansion channel. The sudden expansion channel is assumed to have infinite aspect ratio which is used for the study of the influence of vorticity, and geometric parameters and the angle of attack of VG on fluid flow and heat transfer augmentation without any side wall effect. 47, 93, 140 and 187 are the Re numbers taken for this study as the vortices are steady and discernible only if Re < 1700 [39]. A computational domain of width 80 mm has been considered for the simulation of the laminar and steady flow of water with constant properties due to symmetry of the channel. This is shown in Fig. 1(c). The lengths of upstream and downstream of sudden expansion channel with step height 10 mm are 240 mm and 800 mm ensuring the flow to be fully developed at inlet for a sudden expansion and at outlet of channel. 2D planes have been considered along x, y and z coordinates in the computational domain for interpreting the results of the investigation [11].

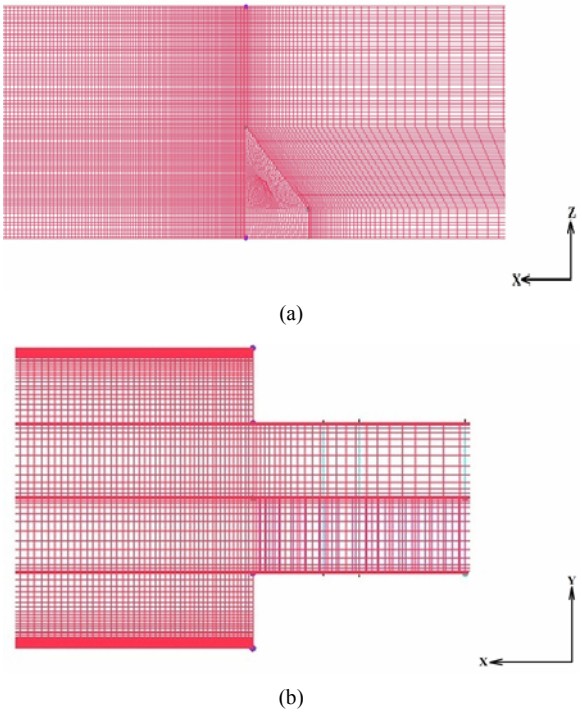

Fig. 2. Mesh details: (a) Around rectangular winglet vortex generator in toe-out configuration at β = 45°; (b) around sudden expansion of the channel.

3. Numerical procedure and validation

3.1 Boundary conditions

A fluid with uniform velocity corresponding to the Re

Table 1. Grid independent study.

Nodes	446453 (Grid 1)	924691 (Grid 2)	1536984 (Grid 3)	2364181 (Grid4)	% Error
Velocity (m/s)	0.002387	0.002429	0.002413	0.002395	0.78
L_{re} (m)	0.0751381	0.0760181	0.0763485	0.0766283	0.37
T_w (K)	307.3925	307.3802	307.3734	307.3685	0.002
Nu	10.327136	10.314085	10.298512	10.257074	0.40

Table 2. Validation for vortex generator.

		G. Zhou et al. (Experimental)	A. Abdollahi et al.	Present study
Re = 650	J/Jo	1.01285	1.106	1.06244
	% Error	-	9.196	4.897
	f/fo	1.40226	1.389	1.26844
	% Error	-	0.946	9.543
Re = 1000	J/Jo	1.08318	1.147	1.08001
	% Error	-	5.892	0.292
	f/fo	1.32081	1.506	1.38961
	% Error	-	14.021	5.209

number considered in this investigation and constant temperature T_{in} = 293 K enters the channel. No slip condition is assumed to be prevailing at all the walls of the channel. Uniform heat flux of 1000 W/m^2 was applied at the bottom wall and all other remaining walls were considered as adiabatic. The existence of fully developed flow at outlet due to long downstream length ensured the outflow condition at the exit.

3.2 Grid independent study and validation

A numerical simulation was carried out to solve continuity Eq. (1), momentum Eq. (2), energy Eq. (3) with gravity and viscous dissipation, and boundary conditions in a commercial CFD code FLUENT 16.2 based on the finite volume method. The computational domain was modeled and segmented into a large number of thin hexahedral elements around walls and corners, and thick hexahedral elements in the remaining region in ICEM CFD for the capture of a precise flow of physics as shown in Figs. 2(a) and (b). SIMPLE algorithm was adapted to couple pressure and velocity using continuity equation. Momentum and energy equations were discretized using second order upwind scheme to get an asymptotic solution of governing equations. Convergence of numerical simulation was decided on the basis of the value of normalized residuals of governing equations and net imbalance across the computational domain in mass and energy rates. The condition for convergence was met when order of scaled residuals of mass, momentum and energy equations was smaller than 10^{-10}, 10^{-10} and 10^{-11}, respectively. The gross imbalance in mass and energy rates were also verified and found to be negligible.

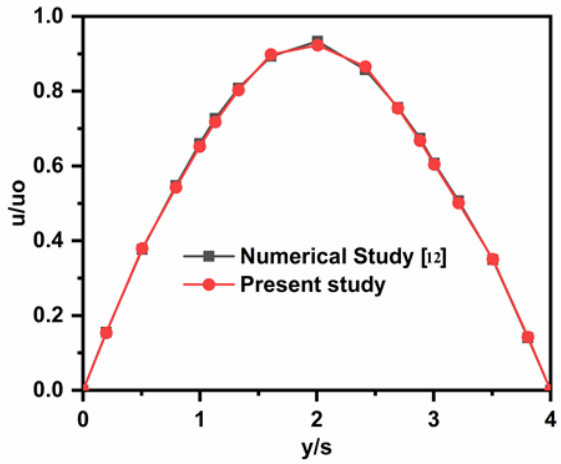

(a)

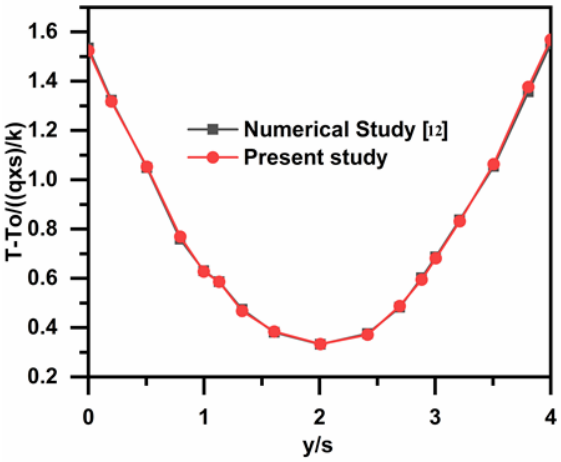

(b)

Fig. 3. Comparison of (a) velocity; (b) temperature between present simulation and numerical simulation [12] for sudden expansion channel.

The governing equations are:

Continuity equation

$$\frac{\partial}{\partial x_k}(\rho \boldsymbol{V}_k) = 0 . \tag{1}$$

Momentum equation

$$\boldsymbol{V}_k \frac{\partial \boldsymbol{V}_j}{\partial x_k} = -\frac{1}{\rho}\frac{\partial P}{\partial x_j} + \nu \frac{\partial}{\partial x_i}\left(\frac{\partial \boldsymbol{V}_i}{\partial x_j} + \frac{\partial \boldsymbol{V}_j}{\partial x_i}\right) + g_j . \tag{2}$$

Energy equation

$$\boldsymbol{V}_k \frac{\partial T}{\partial x_k} = \frac{\nu}{c_v}\left(\frac{\partial \boldsymbol{V}_i}{\partial x_j} + \frac{\partial \boldsymbol{V}_j}{\partial x_i}\right)\frac{\partial \boldsymbol{V}_j}{\partial x_i} + \frac{1}{\rho c_v}\frac{\partial}{\partial x_j}\left(k\frac{\partial T}{\partial x_j}\right). \tag{3}$$

Following are the formulae used to find the simulation results:

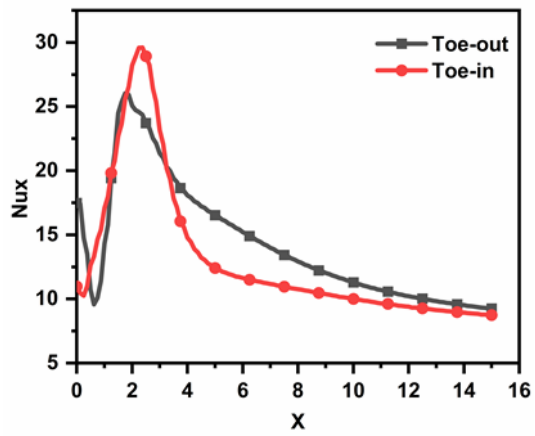

(a)

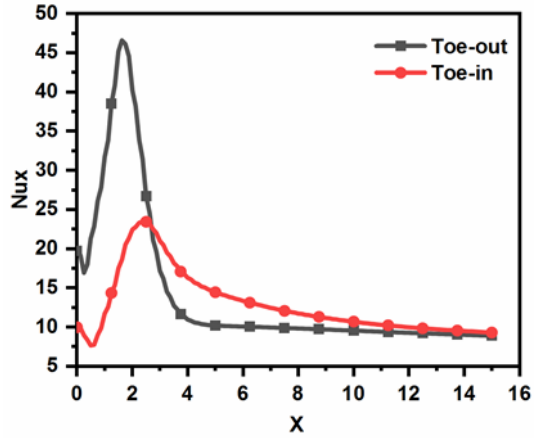

(b)

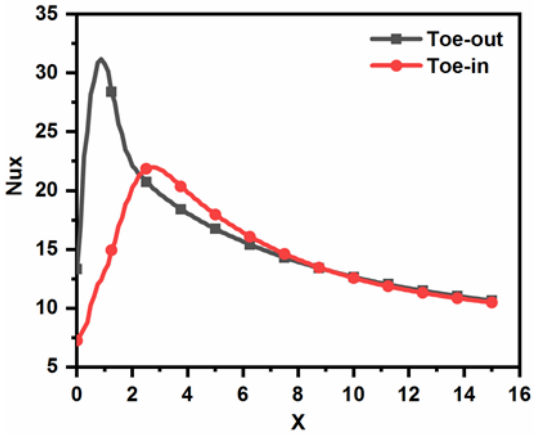

(c)

Fig. 4. Local Nusselt number variation at β = 60° in channel for toe-out and toe-in configurations on plane at (a) z = 20 mm; (b) z = 40 mm; (c) z = 60 mm.

$$Re = \frac{\rho u_o D_h}{\mu}, \tag{4}$$

$$h_c = \frac{q}{(T_w - T_m)}, \tag{5}$$

$$T_m = \frac{T_{in} + T_{out}}{2}, \tag{6}$$

$$Nu = \frac{h_c D_h}{k}, \tag{7}$$

$$Nu_x = \frac{qD_h}{k[T(x)_w - T(x)_b]}, \tag{8}$$

$$T(x)_b = \frac{\Sigma_{i=1}^{n} \rho V_i T_i C}{\rho V_i C}, \tag{9}$$

$$f = \frac{2D_h (P_{in} - P_{out})}{\rho L u_o^2}, \tag{10}$$

$$D_h = \frac{4A}{R}, \tag{11}$$

$$J = \frac{Nu}{Re\, Pr^{1/3}}. \tag{12}$$

An iterating grid-density independence study was performed with four different grid density systems at an angle of attack of 45° for Re = 140 for the choice of a grid volume which would provide a consistent numerical solution of governing equations. Table 1 shows the variations in velocity at x/s = 20, z/w = 0.5 and y/s =1 , reattachment length at z/w = 0.5, wall temperature and Nusselt number calculated during this study, with a difference in those parameters of the third and the fourth grid schemes less than 1 %. The findings of the same numerical simulation procedure followed by Abdollahi et al. [40] and that of experimental study performed by Zhou and Feng [41] have been considered for validating the results of this study. As addressed by Table 2 the results of this study are in good agreement with both experimental and numerical results, and require only a short time to get converged due to hexahedral element throughout the domain. Streamwise velocity and temperature of the flow through sudden expansion channel of the present study at x/s = 64 and z/L = 0.5 are used to compare with those of the numerical simulation carried out by Thiruvengadam et al. [12]. As shown in Figs. 3(a) and (b), the results are in good agreement with an error of less than 1.4 % between them.

4. Results and discussion

4.1 Comparison of heat transfer at β = 60° in toe-out and toe-in configurations

Longitudinal vortices created by baffle in toe-in configuration are perceived to be stronger than those produced in toe-out configuration, leading to a maximum local heat transfer enhancement at z = 20 mm plane as shown in Fig. 4(a) and is vice versa at z = 60 mm plane as shown in Fig. 4(c). Thermal boundary layer thickness is thinner on X = 0.625 plane at z = 20 mm point due to the existence of strong developing longitudinal vortices in toe-in configuration as shown in Fig. 6(a)

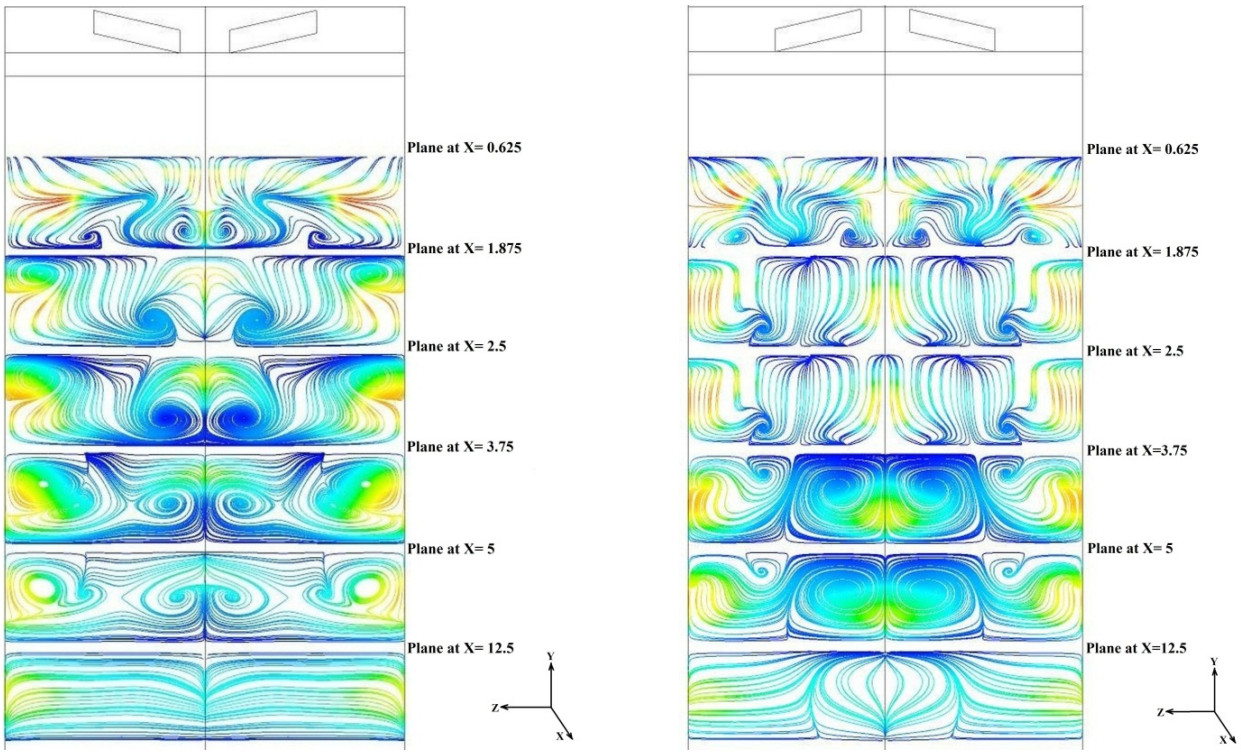

(a) (b)

Fig. 5. Secondary velocity streamline at different locations along the main flow direction at β = 60° for Re = 187 in (a) toe-in; (b) toe-out configurations.

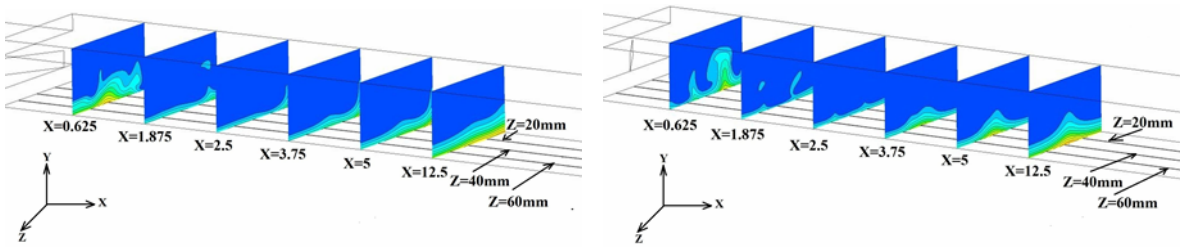

(a) (b)

Fig. 6. Temperature distribution at different locations along the main flow direction at β = 60° for Re = 187 in (a) toe-in; (b) toe-out configurations.

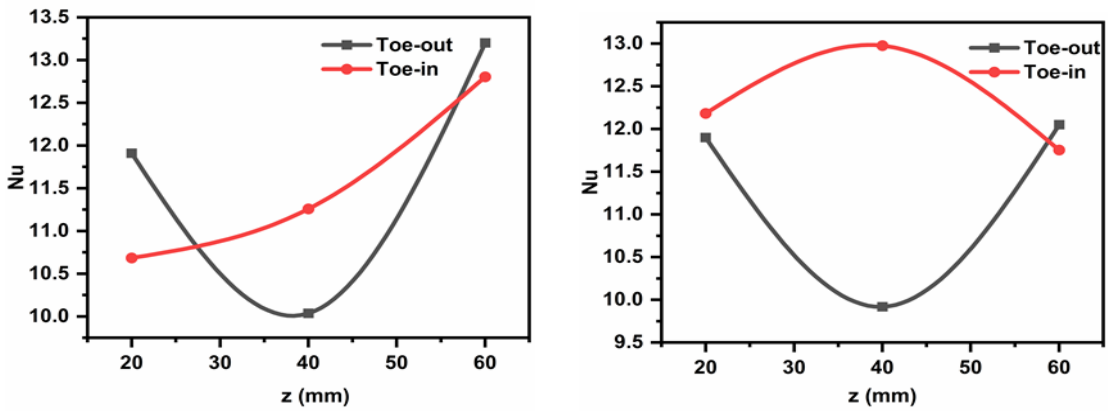

(a) (b)

Fig. 7. Average Nusselt number variation in channel for toe-out and toe-in configurations on plane at z = 20 mm, z = 40 mm and z = 60 mm: (a) At β = 60°; (b) at β = 30°.

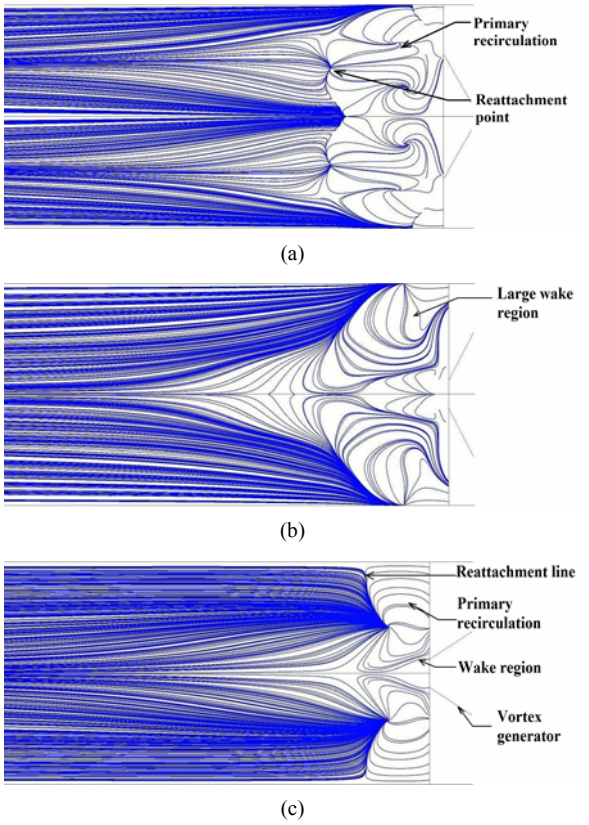

Fig. 8. Limiting velocity streamline distribution for Re = 187: (a) In toe-out configuration at β = 60°; (b) in toe-in configuration at β = 60°; (c) in toe-in configuration at β = 30°.

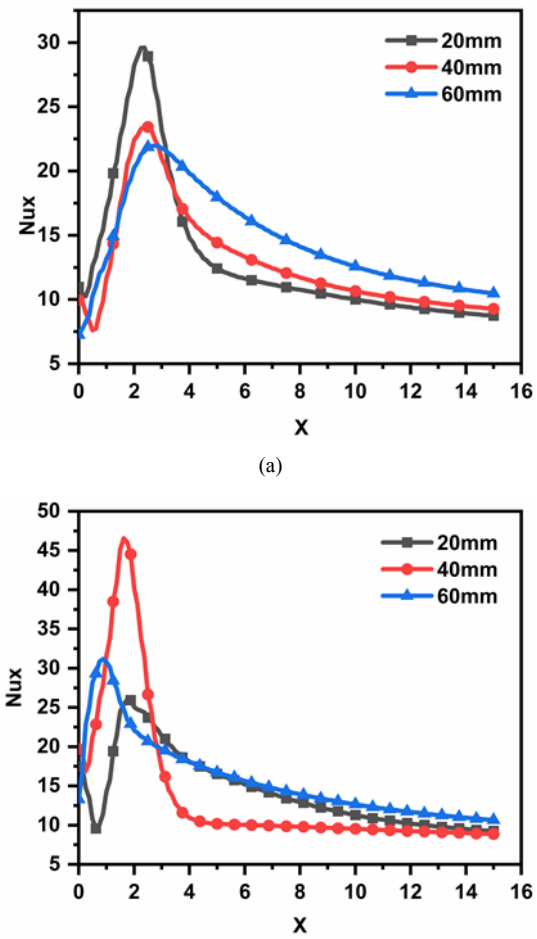

Fig. 9. Local Nusselt number variation in channel at β = 60° on planes at z = 20 mm, z = 40 mm and z = 60 mm for (a) toe-in; (b) toe-out configurations.

comparing to that on the same plane at z = 20 mm point in toe-out configuration as shown in Fig. 6(b) and is vice versa on the same plane at z = 60 mm point. Thermal boundary layer thickness is kept on reducing till a point in the streamwise direction thereafter longitudinal vortices starts loosening its strength leading to the redevelopment of thermal boundary layer in the fully developed flow region in both toe-in and toe-out configurations. Nusselt number on z = 20 mm and z = 40 mm planes initially decreases since the primary recirculation zone is partially lifted off the bottom wall around the step [12, 17]. As the vortices generated in toe-in configuration as depicted in Fig. 5(a), move towards each other, heat transfer rate decreases suddenly on a plane at z = 20 mm after reaching the maximum. Local heat transfer rate increases due to recirculation zone near the step and reaches the maximum around the reattachment point [36, 37], and decreases thereafter on z = 20 mm plane in toe-out configuration. Fig. 5(b) shows longitudinal vortices on z = 20 mm plane in toe-out configuration emerging after a short delay at a point in a streamwise direction augmenting the local heat transfer coefficient better than that in toe-in configuration. This consistent vortex on z = 20 mm plane creates the impression of toe-out configuration being very effective when compared to toe-in configuration in promoting the average heat transfer as shown in Fig. 7(a). The magnitude of maximum local heat transfer depends on both the size of primary recirculation zone and the intensity of secondary vortices. Fig. 8(a) shows the limiting velocity streamlines on a plane (z = 0.0001m) close to the bottom wall providing the local flow structure downstream of sudden expansion. The local flow structure shows size of the recirculation zone behind the VG in toe-out configuration as larger due to the combined effect of primary recirculation and secondary vortices than that in toe-in configuration concluding local heat transfer to be maximum [23] in toe-out configuration at z = 40 mm plane as shown in Fig. 4(b). This is also evident from the temperature plot where thermal boundary layer thickness on X = 0.625 plane at z = 40 mm point in toe-out configuration is thinner than that on the same plane at z = 40 mm point in toe-in configuration. Following the reattachment of fluid on z = 40 mm plane, there was a sudden decrease in the local heat transfer in toe-out configuration. Increase in local convective heat transfer coefficient on z = 40 mm plane in toe-in configuration was seen, reaching the maximum around the reattachment point. There was a decrease thereafter, but the rate of decrease in heat transfer coefficient was less than that in toe-out con-

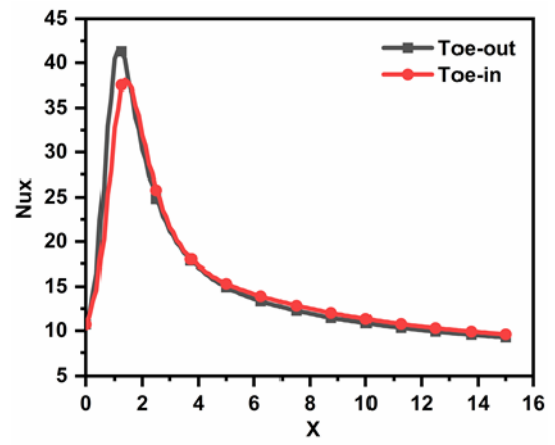

(a)

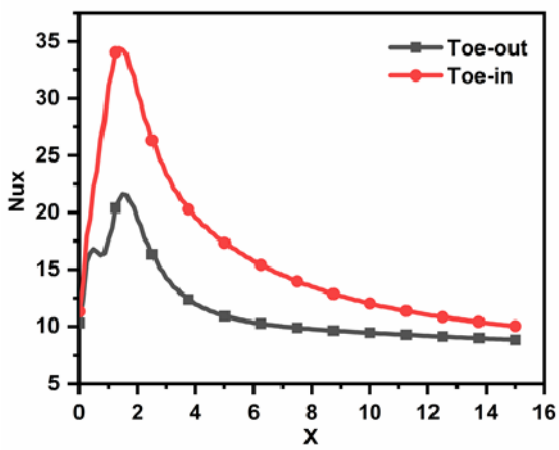

(b)

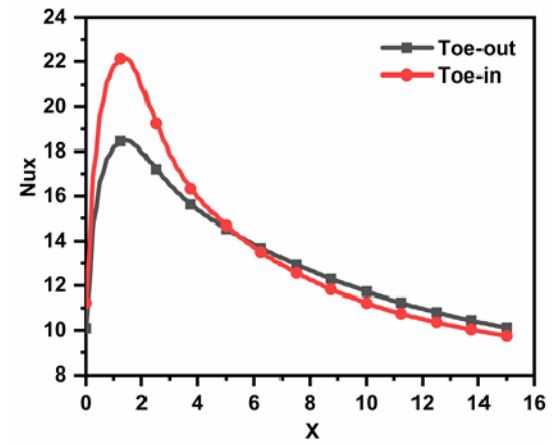

(c)

Fig. 10. Local Nusselt number variation at β = 30° in channel for toe-out and toe-in configurations on plane at (a) z = 20 mm; (b) z = 40 mm; (c) z = 60 mm.

figuration due to the influence of secondary flow created at z = 60 mm plane as shown in Fig. 5(a) making toe-in configuration better in overall heat transfer enhancement as shown in Fig. 7(a).

Fig. 8(b) shows wake region (Von Karman vortex) as predominating at z = 60 mm plane. The presence of large wake region [31, 32] over z = 60 mm plane, led to the observation of heat transfer enhancement as relatively poor in toe-in configuration. The secondary vortex flow at z = 60 mm plane along with above discussed reasons could be ascribed to the best performance of VG at β = 60° in toe-out configuration for Re = 187 as shown in Fig. 7(a).

4.2 Heat transfer at β = 60° in toe-in configuration

Fig. 9(a) shows heat transfer rate as maximum at a point where the fluid is reattached to the bottom wall in the downstream. This maximum local heat transfer rate is relatively high when compared to that on planes at z = 40 mm and 60 mm as the length of primary recirculation is very large [23] on plane at z = 20 mm. The maximum heat transfer enhancement on planes at z = 20 mm, 40 mm and 60 mm takes the order of preferences with respect to its reattachment length; reattachment on z = 20 mm being the largest and that on z = 60 mm being the smallest. Though the maximum local heat transfer coefficient on z = 60 mm is very low due to its short reattachment length, its average Nusselt number is significantly greater than that on z = 20 mm due to its consistent strong secondary vortex flow.

4.3 Heat transfer at β = 60° in toe-out configuration

Fig. 9(b) depicts the increase in local heat transfer rate as a result of the presence of recirculation zone near the step reaching the maximum around the reattachment point on z = 20 mm plane. But, the delayed development of secondary vortex in streamwise direction around x = 130 mm caused the impression of the local heat transfer being better than that at z = 40 mm plane. The large size primary recirculation flow right behind the VG caused increase in local Nusselt number to a high value around a point where the flow reattached and dropped suddenly thereafter at z = 40 mm plane. As the longitudinal vortices were very strong on z = 60 mm plane, the average Nusselt number appeared to be better when compared to that on planes at z = 20 mm and 40 mm.

4.4 Comparison of heat transfer at β = 30° in toe-out and toe-in configurations

Due to the presence of wake region behind VG at β = 30° in toe-in configuration as depicted in Fig. 8(c), the local maximum heat transfer coefficient is smaller than that in toe-out configuration at a plane z = 20 mm as shown in Fig. 10(a). But, Fig. 7(b) shows the average Nusselt number on that plane z = 20 mm in toe-in configuration as greater than that in toe-out configuration owing to the strong secondary vortex flow. Though the core centers of vortices move towards each other and lift away from the bottom wall as shown in Figs. 11(a) [38] and (b) in toe-in and toe-out configurations respectively and as the strong secondary vortex expands in a transverse

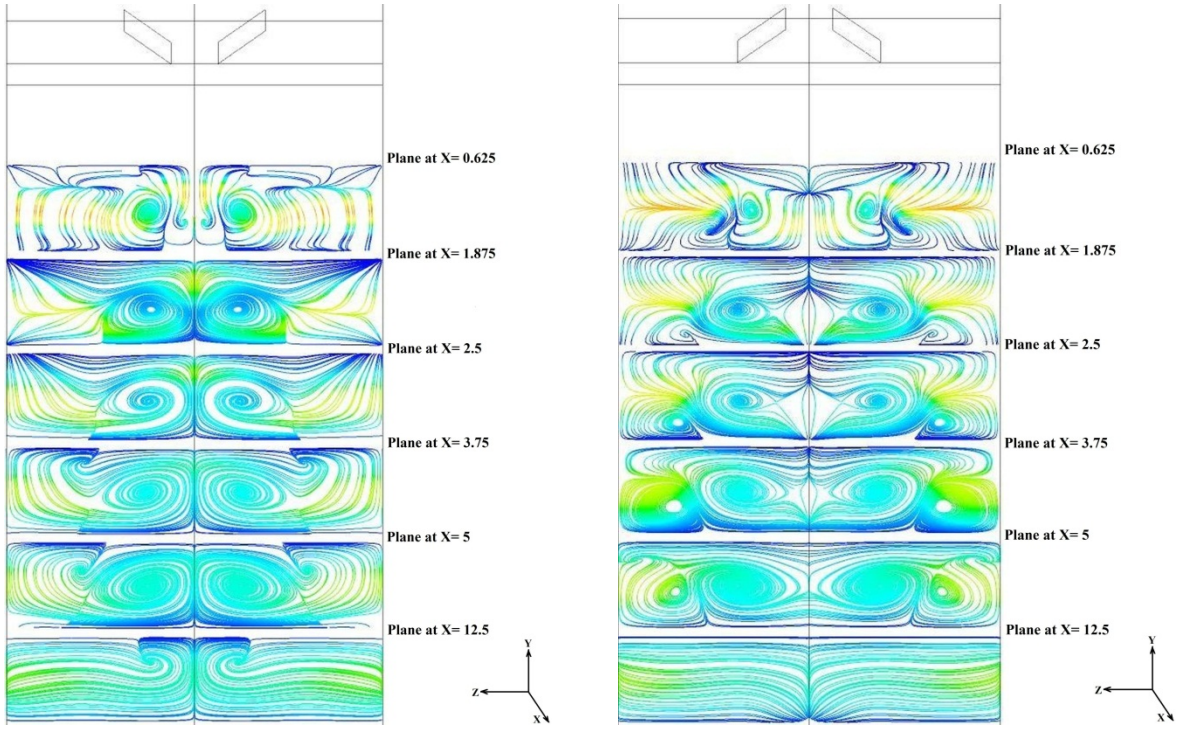

Fig. 11. Secondary velocity streamline at different locations along the main flow direction at β = 30° for Re = 187 in (a) toe-in; (b) toe-out configurations.

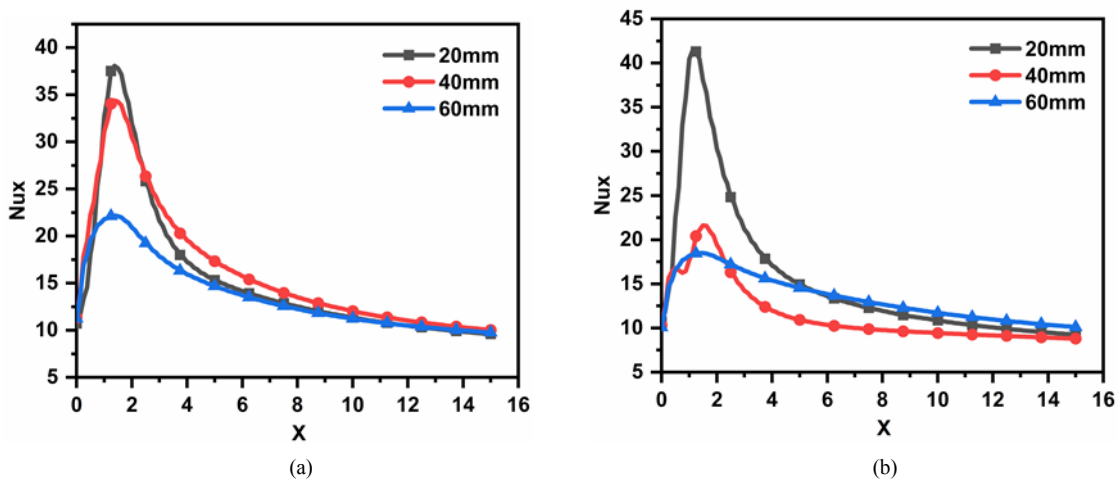

Fig. 12. Local Nusselt number variation in channel at β = 30° on planes at z = 20 mm, z = 40 mm and z = 60 mm for (a) toe-in; (b) toe-out configurations.

direction in the toe-in configuration, the local and average Nusselt number in toe-in configuration on a plane at z = 40 mm were found to be very much superior to that in toe-out configuration as depicted in Figs. 10(b) and 7(b), respectively. Fig. 7(b) shows the average Nusselt number on z = 60 mm plane in toe-out configuration as slightly more than that in toe-in configuration as the streamwise velocity of fluid in toe-out configuration was high, though local heat transfer enhancement trend in toe-in configuration had the peak value as shown in Fig. 10(c) due to the effect of secondary vortex expansion in lateral direction. Thus the secondary vortex flow created in the region around z = 20 mm plays a vital role in making toe-in configuration better in heat transfer enhancement than toe-out configuration at β = 30° for Re = 187.

4.5 Heat transfer at β = 30° in toe-in configuration

A high intensity secondary vortex flow was generated at β =

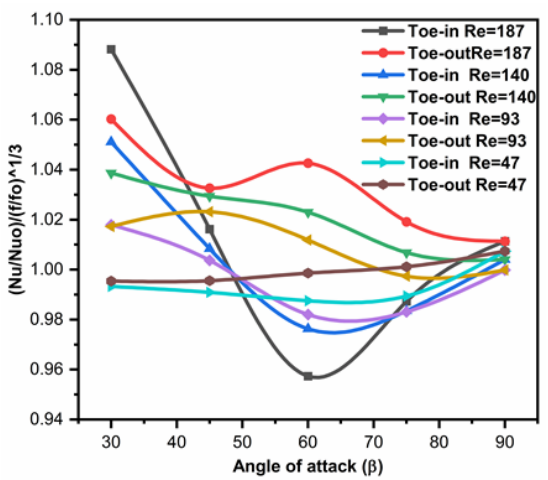

Fig. 13. Performance comparison of channels with VGs.

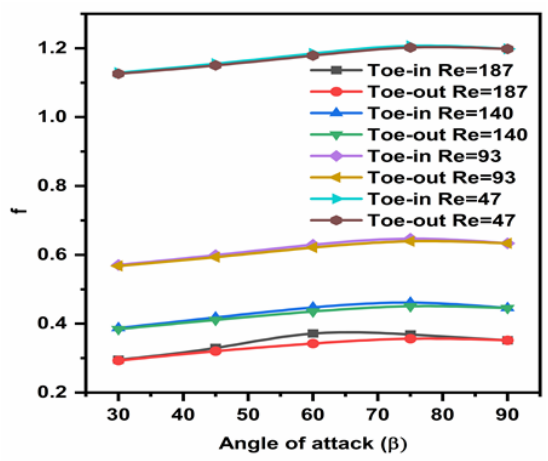

Fig. 14. Variation of the friction factor versus the angle of attack at different Reynolds numbers.

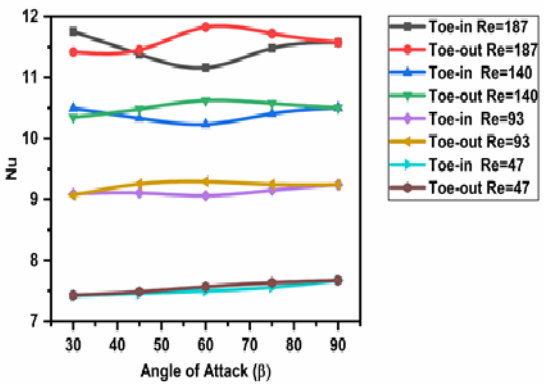

Fig. 15. Variation of average Nusselt number versus the angle of attack at different Reynolds numbers.

30°. It had a high influence on the flow on a plane around z = 20 mm. Due to this swirling flow, maximum local heat transfer coefficient was large when compared to that on planes at z = 40 mm and 60 mm as shown in Fig. 12(a).

As the vortex on z = 20 mm plane expanded in the spanwise direction along x direction [40] as depicted in Fig. 11(a), local Nusselt number on z = 40 mm plane exceeded that on z = 20 mm plane at x = 100 mm. Local heat transfer coefficient on z = 60 mm plane was very poor as the main flow in this region did not entrain any secondary vortex flow and that, on all the planes at z = 20 mm, 40 mm, and 60 mm was maximum at around their respective reattachment points. Core centers of the secondary vortex flow moved towards each other and away from the bottom wall as the flow proceeded along x direction in the toe-in configuration. Average Nusselt numbers on planes at z = 20 mm and 40 mm were greater than those at z = 60 mm plane due to the presence of a strong secondary vortex flow making toe-in configuration superior in heat transfer enhancement to toe-out configuration.

4.6 Heat transfer at β = 30° in toe-out configuration

Secondary flow generated by LVG at β = 30° was very dominant on a plane at z = 20 mm causing rapid enhancement of the heat transfer rate as depicted in Fig. 12(b). When this longitudinal vortex moved further in a streamwise direction, it shed a new corner vortex [31] by imparting its angular momentum, thereby losing its intensity as shown in Fig. 11(b). Longitudinal vortex shed by VG moved in the lateral direction towards z = 40 mm plane in the downstream giving a local maximum heat transfer enhancement on a plane at z = 40 mm. As most of regions around z = 40 mm plane lay in the interface between the two counter rotating vortices, the average heat transfer enhancement in this region was very poor. Despite the initial increase in the local heat transfer coefficient, it started decreasing gradually after reaching the local maximum around reattachment on plane at z = 60 mm. Due to the spiral motion imparted by the vortices from z = 20 mm plane and its entrainment by high velocity main flow at z = 60 mm plane, the average heat enhancement appeared to be better than that on plane at z = 40 mm as shown in Fig. 7(b). Heat transfer enhancement and fluid flow structure discussed so far relate only to the angle of attacks (β = 30° and β = 60°) which was observed to be most suitable for a good performance of VGs. The flow physics interpreted for β = 30° and β = 60° can also be applied to the remaining angle of attack and is not present here due to space limitations.

4.7 Overall performance at various angle of attack

Longitudinal VGs promote not only heat transfer, but also pressure loss. So a performance evaluation parameter $(Nu/Nuo)/(f/fo)^{1/3}$ has been considered for the quantification of the overall performance of LVG in augmenting the heat transfer against pressure loss [42, 43], to find out the best condition where adoption of LVG could be most appropriate. As Fig. 13 reveals RWVGs in toe-out configuration as appearing to have better overall performance over a wide range of angle of attack for a given Re number [38]. RWVGs in toe-out configu-

ration are very much superior to those in toe-in configuration especially at high Re number and at β = 60°. Due to the presence of strong secondary vortex and low form drag at higher Re numbers, RWVG at β = 30° and β = 45° respectively were seen providing the best and a better overall performance in both toe-in and toe-out configurations. RWVG at β = 60° and β = 75° in toe-in configuration is not at all suitable for promoting heat transfer as it demands more frictional loss at the same pumping power. At low Re number, overall performance of RWVG in toe-in and toe-out configurations is less than unity almost over a wide range of angle of attack indicating that RWVG accompanies more frictional loss than heat transfer enhancement.

4.8 Average friction factor at various angle of attack

With decrease in the thickness of hydrodynamic boundary layer at a high Re number, the fluid experienced low friction, in turn increasing with increase in the angle of attack due to form drag [40, 44] and transverse expansion of longitudinal vortices [45] as depicted in Fig. 14. The rate of increase in friction factor increased with decrease in velocity for all angles of attack.

4.9 Average Nusselt number at various angle of attack

Heat transfer enhancement in toe-out configuration is better than toe-in configuration at all angles of attack analyzed when Re number is low, but at high Re number as a strong vortex is present at β = 30°, toe-in is observed to be better than toe-out instead of being inferior to toe-out at all angles of attack as shown in Fig. 15. Average Nusselt number is maximum at β = 60° for all Re numbers [46] studied in toe-out configuration.

5. Conclusion

In the present investigation, a three dimensional numerical simulation was performed on a sudden expansion channel with rectangular winglet vortex generators in toe-out and toe-in configurations for a study of the heat transfer enhancement and local flow structure and a comparison between them. The following are the major conclusions drawn from this study.

Rectangular winglet vortex generators in toe-out configuration have a better overall performance than that in toe-in configuration over the range of Re number discussed and are very much superior to those in toe-in configuration especially at high Re number and at $\beta = 60^o$.

Irrespective of configurations, rectangular winglet vortex generators are found to have better overall performance at $\beta = 30^o$ and $\beta = 45^o$ in both toe-out and toe-in configurations due to strong secondary vortex flow.

Rectangular winglet vortex generators are seen providing effective enhancement of heat transfer at $\beta = 30^o$ and $\beta = 60^o$ in toe-in and toe-out configurations, respectively.

With rectangular winglet vortex generators, friction factor increases with increase in angle of attack and decrease in Re number.

Nomenclature

a	: Transverse distance between the VGs (m)
A	: Cross sectional area of channel at inlet (m^2)
C	: Height of computational cell (or) grid (m)
CRWVG	: Curved rectangular winglet vortex generator
CDWVG	: Curved delta winglet vortex generator
D_h	: Hydraulic diameter (m)
f	: Friction factor
g	: Gravity acceleration (m/s^2)
H	: Downstream channel height (m)
h	: Upstream channel height (m)
h_c	: Heat transfer coefficient (W/m^2K)
J	: Colburn factor
k	: Thermal conductivity (W/mK)
L	: Downstream channel length (m)
l	: Upstream channel length (m)
Nu	: Average Nusselt number
Nu_x	: Local Nusselt number
P	: Pressure (N/m^2)
Pr	: Prandtl number
q	: Heat flux (W/m^2)
R	: Perimeter of channel at inlet (m)
Re	: Reynolds number
S	: Step height (m)
T	: Temperature (K)
T_o	: Inlet temperature (K)
u	: Velocity (m/s)
u_o	: Inlet velocity
V	: Velocity vector
VG	: Vortex generator
W	: Width of the channel (m)
X	: Non-dimensional length
x, z	: Cartesian coordinate (m)

Greek symbol

β	: Angle of attack (^{o})
ρ	: Density (kg/m^3)
Cv	: Specific heat at constant volume (J/kg K)
μ	: Viscosity (Ns/m^2)
ν	: Kinematic viscosity (m^2/s)

Subscripts

b	: Bulk
i, k	: Index
in	: Inlet
m	: Average
o	: Free stream
out	: Outlet
w	: Wall

References

[1] A. E. Bergles, *Hanbook of Heat Transfer*, 3rd Edition, McGraw-Hill, New York, NY, USA (1998).

[2] A. E. Bergles, The implications and challenges of enhanced heat transfer for the chemical process industries, *Chemical Engineering Research and Design*, 79 (2001) 437-444.

[3] S. A. E. Sayed Ahmed, E. Z. Ibrahiem, O. M. Mesalhy and M. A. Abdelatief, Heat transfer characteristics of staggered wing-shaped tubes bundle at different angle of attack, *Heat Mass Transfer*, 50 (2014) 1091-1102.

[4] S. A. E. Sayed Ahmed, E. Z. Ibrahiem, O. M. Mesalhy and M. A. Abdelatief, Effect of attack and cone angles on air flow characteristics for staggered wing-shaped tubes bundles, *Heat Mass Transfer*, 51 (2015) 1001-1016.

[5] S. A. E. Sayed Ahmed, O. M. Mesalhy and M. A. Abdelatief, Flow and heat transfer enhancement in tube heat exchangers, *Heat Mass Transfer*, 51 (2015) 1607-1630.

[6] A. Dewan, P. Mahanta, K. Sumithra Raju and P. Suresh Kumar, Review of passive heat transfer augmentation techniques, *Proc. Instn. Mech. Engrs. Part A: J. Power and Energy*, 218 (7) (2004) 509-527.

[7] S. A. E. Sayed Ahmed, O. M. Mesalhy and M. A. Abdelatief, Heat transfer characteristics and entropy generation for wing-shaped-tubes with longitudinal external fins in cross-flow, *Journal of Mechanical Science and Technology*, 30 (6) (2016) 2849-2863.

[8] M. A. Abdelatief, S. A. E. Sayed Ahmed and O. M. Mesalhy, Experimental and numerical study on thermal-hydraulic performance of wing-shaped-tubes-bundle equipped with winglet vortex generators, *Heat Mass Transfer*, 54 (2018) 727, 744.

[9] E. Schreck and M. Scha, Numerical study of bifurcation in three-dimensional sudden channel expansions, *Computers & Fluids*, 29 (2000) 583-593.

[10] R. C. Lima, C. R. Andrade and E. L. Zaparoli, Numerical study of three recirculation zones in the unilateral sudden expansion flow, *Int. Commun. Heat Mass Transf.*, 35 (9) (2008) 1053-1060.

[11] P. S. B. Zdanski and M. Vaz Jr., Three-dimensional polymer melt flow in sudden expansions: Non-isothermal flow topology, *Int. J. Heat Mass Transf.*, 52 (2009) 3585-3594.

[12] M. Thiruvengadam, J. H. Nie and B. F. Armaly, Bifurcated three-dimensional forced convection in plane symmetric sudden expansion, *Int. J. Heat Mass Transf.*, 48 (2005) 3128-3139.

[13] M. Thiruvengadam, B. F. Armaly and J. A. Drallmeier, Three dimensional mixed convection in plane symmetric-sudden expansion: Symmetric flow regime, *Int. J. Heat Mass Transf.*, 52 (2009) 899-907.

[14] J. Paik and F. Sotiropoulos, Numerical simulation of strongly swirling turbulent flows through an abrupt expansion, *International Journal of Heat and Fluid Flow*, 31 (3) (2010) 390-400.

[15] T. Balakhrisna, S. Ghosh, G. Das and P. K. Das, Oil-water flows through sudden contraction and expansion in a horizontal pipe - Phase distribution and pressure drop, *Int. J. Multiphase Flow*, 36 (1) (2010) 13-24.

[16] D. S. Christopher, G. R. Madhusudhana, P. Venkumar, P. R. Kanna and H. A. Mohammed, Numerical investigation on laminar forced convection flow due to sudden expansion using nanofluids, *J. Computational and Theoretical Nanoscience*, 9 (12) (2012) 1-11.

[17] D. H. Lee, H. J. Park and S. J. Kim, Local heat transfer downstream of an asymmetric abrupt expansion and cavity in a circular tube, *Int. J. Therm. Sci.*, 79 (2014) 229-239.

[18] W. Cherdron, F. Durst and J. Whitelaw, Asymmetric flows and instabilities in symmetric ducts with sudden expansions, *J. Fluid Mech.*, 84 (1978) 13-31.

[19] Y. Ouwa, M. Watanabe and H. Asawo, Flow visualization of a two-dimensional water jet in a rectangular channel, *J. Appl. Phys.*, 20 (1) (1981) 243-247.

[20] T. P. Chiang, T. W. H. Sheu and S. K. Wang, Side wall effects on the structure of laminar flow over aplane-symmetric sudden expansion, *Computers & Fluids*, 29 (2000) 467-492.

[21] X.-R. Zhang, B.-L. Deng and H. Yamaguchi, Bifurcation phenomenon for force convection of supercritical CO_2 sudden expansion flow and heat transfer in symmetric regime, *Int. J. Heat Mass Transf.*, 53 (2010) 4467-4473.

[22] P. Rajesh Kanna, J. Taler, V. Anbumalar, A. V. Santhosh Kumar, A. Pushparaj and D. S. Christopher, Conjugate heat transfer from sudden expansion using nanofluid, *Numerical Heat Transfer, Part A*, 67 (2015) 75-99.

[23] H. Togun, H. I. Abu-Mulaweh, S. N. Kazi and A. Badarudin, Numerical simulation of heat transfer and separation Al_2O_3/nanofluid flow in concentric annular pipe, *International Communications in Heat and Mass Transfer*, 71 (2016) 108-117.

[24] A. Kimouche, A. Mataoui, H. F. Oztop and N. Abu-Hamdeh, Analysis of heat transfer of different nanofluids flow through an abrupt expansion pipe, *Applied Thermal Engineering*, 112 (2017) 965-974.

[25] B. Gong, L.-B. Wang and Z.-M. Lin, Heat transfer characteristics of a circular tube bank fin heat exchanger with fins punched curve rectangular vortex generators in the wake regions of the tubes, *Applied Thermal Engineering*, 75 (2015) 224-238.

[26] Z.-M. Lin, C.-P. Liu, M. Lin and L.-B. Wang, Numerical study of flow and heat transfer enhancement of circular tube bank fin heat exchanger with curved delta-winglet vortex generators, *Applied Thermal Engineering*, 88 (2015) 198-210.

[27] X. Wu, Z.-M. Lin, S. Liu, M. Su, L.-C. Wang and L.-B. Wang, Experimental study on the effects of fin pitches and tube diameters on the heat transfer and fluid flow characteristics of a fin punched with curved delta-winglet vortex generators, *Applied Thermal Engineering,* 119 (2017) 560-572.

[28] W. Dang, J. Nugud, Z.-M. Lin, Y.-H. Zhang, S. Liu and L.-B. Wang, The performances of circular tube bank fin heat exchangers with fins punched with quadrilateral vortex generators and flow re-distributors, *Applied Thermal Engineering*, 134 (2018) 437-449.

[29] M. Hatami, D. D. Ganji and M. Gorji-Bandpy, Experimental investigations of diesel exhaust exergy recovery using delta winglet vortex generator heat exchanger, *International Journal of Thermal Sciences*, 93 (2015) 52-63.

[30] J. S. Yang, D. W. Lee and G. M. Choi, Numerical investiga-

tion of fluid flow and heat transfer characteristics by common-flow-up, *International Journal of Heat and Mass Transfer*, 51 (2008) 6332-6336.

[31] A. Arora, P. M. V. Subbarao and R. S. Agarwal, Numerical optimization of location of 'common flow up' delta winglets for inline aligned finned tube heat exchanger, *Applied Thermal Engineering*, 82 (2015) 329-340.

[32] A. Pal, D. Bandyopadhyay, G. Biswas and V. Eswaran, Enhancement of heat transfer using delta-winglet type vortex generators with a common-flow-up arrangement, *Numerical heat transfer, Part A: Applications: An International Journal of Computation and Methodology*, 61 (12) 912-928.

[33] S. M. Pesteei, P. M. V. Subbarao and R. S. Agarwal, Experimental study of the effect of winglet location on heat transfer enhancement and pressure drop in fin-tube heat exchangers, *Applied Thermal Engineering*, 25 (2005) 1684-1696.

[34] L. Li, X. Du, Y. Zhang, L. Yang and Y. Yang, Numerical simulation on flow and heat transfer of fin-and-tube heat exchanger with longitudinal vortex generators, *International Journal of Thermal Sciences*, 92 (2015) 85-96.

[35] A. Bekele, M. Mishra and S. Dutta, Performance characteristics of solar air heater with surface mounted obstacles, *Energy Conversion and Management*, 85 (2014) 603-611.

[36] A. E. Zohir, A. A. Abdel Aziz and M. A. Habib, Heat transfer characteristic in a sudden expansion pipe equipped with swirl generators, *Int. J. Heat Fluid Flow*, 32 (2011) 352-361.

[37] A. E. Zohir and A. G. Gomaab, Heat transfer enhancement through sudden expansion pipe airflow using swirl generator with different angles, *Exp. Therm. Fluid Sci*., 45 (2013) 146-154.

[38] L.-T. Tian, Y.-L. He, Y.-G. Lei and W.-Q. Tao, Numerical study of fluid flow and heat transfer in a flat-plate channel with longitudinal vortex generators by applying field synergy principle analysis, *International Communications in Heat and Mass Transfer*, 36 (2009) 111-120.

[39] S. Tiggelbeck, N. Mitra and M. Fiebig, Flow structure and heat transfer in a channel with multiple longitudinal vortex generators, *Exp. Therm. Fluid Sci*., 5 (1992) 425-436.

[40] A. Abdollahi and M. Shams, Optimization of shape and angle of attack of winglet vortex generator in a rectangular channel for heat transfer enhancement, *Appl. Therm. Eng*., 81 (2015) 376-387.

[41] G. Zhou and Z. Feng, Experimental investigation of heat transfer enhancement by plane and curved winglet type vortex generators with punched holes, *Int. J. Therm. Sci*., 78 (2014) 26-35.

[42] M. A. Omara and M. A. Abdelatief, Experimental study of heat transfer and friction factor inside elliptic tube fixed with helical coils, *Appl. Therm. Eng*., 134 (2018) 407-418.

[43] M. A. E. Sayed Ahmed, E. Z. Ibrahim, M. M. Ibrahim, M. A. Essa, M. A. Abdelatief and M. N. El-Sayed, Heat transfer performance evaluation in circular tubes via internal repeated ribs with entropy and exergy analysis, *Appl. Therm. Eng*., 144 (2018) 1056-1070.

[44] Y. Chen, M. Fiebig and N. K. Mitra, Heat transfer enhancement of a finned oval tube with punched longitudinal vortex generators in line, *Int. J. Heat Mass Transf*., 41 (1998) 4151-4166.

[45] J. S. Wang, J. J. Tang and J. F. Zhang, Mechanism of heat transfer enhancement of semi-ellipse vortex generator, *J. Mech. Eng*., 42 (5) (2006) 160-164.

[46] T. Alam, R. P. Saini and J. S. Saini, Effect of circularity of perforation holes in V-shaped blockages on heat transfer and friction characteristics of rectangular solar air heater duct, *Energy Convers Manage*, 84 (2014) 952-963.

Seranthian Ramanathan has 10 years of experience in teaching thermal and fluid engineering related subjects. He is currently working on sudden expansion, and vortex generators .

M. R. Thansekhar is a Professor of Mechanical Engineering and Convener of Quality Circle for Advanced Research and Development at K.L.N. College of Engineering, Madurai, Tamilnadu, India. He graduated from P.S.G. College of Technology, Coimbatore, India and received his Ph.D degree from Indian Institute of Technology Madras [IIT-M], Chennai, India. His research interest includes numerical and experimental heat transfer, microchannel flows, friction stir welding and optimization.

Rajesh Kanna, M.E., Ph.D., D.Sc., Associate Professor and Head of Dept. of Mechanical Engineering, CEC, has joined Sep. 2017 CEC, AGU. He has obtained his Ph.D. from Indian Institute of Technology Guwahati in the year 2006 and Doctor of Science from Cracow University of Technology, Poland on May 2015. His area of specialization is fluid-thermal engineering and he has published more than 50 research papers in the reputed journals and presented 20 papers in the conferences. He has guided Ph.D. scholars in the area of jet flow, nanofluid heat transfer, bluff body simulation, natural convection in a cavity.

Prem Gunnasegaran is a Senior Lecturer at the Universiti Tenaga Nasional (UNITEN), Selangor, Malaysia. He received his Ph.D in 2016 from the Universiti Sains Malaysia, Penang, Malaysia. He is the Manager of Research Centre of Fluid Dynamics at College of Engineering, UNITEN. He has been teaching at the UNITEN since 2009. He is currently working on enhanced heat transfer in heat pipes under numerical and experimental aspects.